

# Light and Electron Microscopic Study on the Effect of Gibberellic Acid on the Renal Cortex of Adult Male Albino Rats and the Possible Protective Role of Coenzyme Q10

Original  
Article

Amira Fahmy Ali<sup>1</sup>, Nagwa Saad Ghoneim<sup>1</sup> and Rasha M. Salama<sup>2</sup>

<sup>1</sup>Department of Histology, <sup>2</sup>Department of Anatomy and Embryology, Faculty of Medicine; Menoufia University

## ABSTRACT

**Background:** Gibberellic acid (GA3) is considered one of the plant growth regulators (PGRs), utilized to increase the production, size and availability of the plants all the year. however, it should be utilized guardedly to reduce its prospective toxicity on body organs involving the kidney. Coenzyme Q10 (CoQ10) is present naturally in the body as a nutrient. It occurs also in multiple foods and has an antioxidant action, which inhibits cell damage and has an important role in metabolism.

**Objective:** The target of this work is to estimate the impact of GA3 on the rat's renal cortex and the potential protective effect of CoQ10.

**Materials and Methods:** Forty male albino rats were used in the current work. The animals were divided into control group, CoQ10 treated group, GA3 treated group and finally, CoQ10 and GA3 treated group. After 4 weeks, urea and creatinine levels were measured in the blood and kidney tissues were processed for biochemical, light and electron microscopic studies.

**Results:** GA3 treated group revealed marked glomerular and tubular damage. Thickened glomerular basement membrane, glomerular atrophy and increased tubular diameter were evident. There were some tubular cells with cytoplasmic vacuoles and pyknotic nuclei. Hyalinization of the lumen of some renal tubules was noticed. The interstitium revealed heavy cellular infiltration and blood congestion. Biochemical study, revealed a marked increase in plasma levels of urea and creatinine, increased malondialdehyde (MDA) and a marked decrease in the catalase (CAT) and superoxide dismutase (SOD) levels compared to control group. These changes were ameliorated by CoQ10.

**Conclusion:** Administration of CoQ10 protect against GA3 induced renal damage.

**Received:** 20 May 2020, **Accepted:** 25 July 2020

**Key Words:** Coenzyme Q10, desmin, gibberellic acid, kidney.

**Corresponding Author:** Amira Fahmy Ali, MD, Department of Histology, Faculty of Medicine; Menoufia University, Egypt, Tel.: +20 1068915402, E-mail: amirafahmy356@yahoo.com

ISSN: 1110-0559, Vol. 44, No.2

## INTRODUCTION

Gibberellic acid (GA3) is considered one of the plant growth regulators (PGRs) which were first reported in 1930s<sup>[1]</sup> and used in agriculture to enhance and regulate the production of a wide variety of crops<sup>[2]</sup>. According to the American Society of Agricultural Science, one of the six major classes of PGRs is Gibberellins<sup>[1]</sup>.

GA3 can be considered as the most active hormones of gibberellins affecting cell division, leaves and stems elongation leading to flowering and fruit development<sup>[3]</sup>.

GA3 used widely in Egypt to increase the growth of various fruits and vegetables as grapes, strawberries, tomatoes, cauliflower and cabbages<sup>[4]</sup>. Exposure to GA3 may be through consumption of fruits and vegetables treated with it, or through agricultural workers inhalation and dermal contact<sup>[5]</sup>.

GA3-treated cells are unable to scavenge reactive oxygen species resulting in oxidative damage and stress that leads to damage of cells in various organs like the spleen, liver, kidney, stomach, and heart through generation of free radicals<sup>[6]</sup>.

Coenzyme Q10 (CoQ10 or ubiquinone) is an endogenous lipid and a free radicals scavenger natural antioxidant. It can be obtained from consumption of fruits, vegetables, fish, meat, and poultry, however most healthy people have enough CoQ10 naturally<sup>[7]</sup>. Increasing age and some medical conditions are associated with dropping its level.

Adding more CoQ10 supplements may be beneficial<sup>[8]</sup>.

It is an oil soluble vitamin-like substance, found in the membranes of many organelles, and used as an electron carrier in aerobic cellular respiration for energy generation as it is a component of the electron transport chain<sup>[9]</sup>.

CoQ10 has been used to treat many different conditions, it can be used to lower blood pressure and to treat heart failure, migraine headaches, low sperm count and gum diseases. It could also, reduce the oxidative damage that leads to skin damage, muscle fatigue and lung diseases and many other conditions<sup>[10]</sup>. Therefore, this study pointed to estimate the effect of GA3 on the rat's renal cortex and the potential protective effect of CoQ10.

## MATERIALS AND METHODS

### *Drugs and chemicals*

Gibberellic acid (GA3): It is available as vials. Each vial contained one gm of GA powder, manufactured by Sigma Company (St. Louis, Mo, USA).

Coenzyme Q10 (CoQ10): It is available as capsules (30mg), manufactured by Mepaco-Arab company for Pharmaceuticals and Medicinal Plant.

### *Animals*

Forty adult male albino rats, weighing 170-200 g and of 3 months of age were used in the current work. The rats were housed in properly ventilated cages with controlled temperature (25 °C), humidity and 12h light /dark cycles. The rats were allowed free access to water and food. Strict hygiene was followed to keep a healthy medium for rats. All animals protocols were authorized and observed via the Animal Care Committee of the Research Laboratory of Experimental Animals at Faculty of Medicine, Menoufia university, Egypt.

### *Experimental protocol*

The animals were divided into four groups, each included 10 rats.

Group I (control group): The rats received 1ml distilled water by oral intubation once daily for four weeks.

Group II (CoQ10 treated group): The rats received coenzyme Q10, 4 mg/kg/d by oral intubation for 4 weeks<sup>[11]</sup>.

Group III (GA3 treated group): The rats received GA3, 20 mg/Kg/d that was dissolved in distilled water by oral intubation for 4 weeks<sup>[12]</sup>.

Group IV (CoQ10 and GA3 treated group): The animals in this group received coenzyme Q10 and GA3, with the same doses and duration as groups II & III respectively.

24 h after the last dose of drugs administration, ether inhalation was used to anaesthetize the rats from all groups. Blood samples were obtained from the retro-orbital plexus and then, collected into heparin coated tubes and centrifuged for biochemical analysis. The kidney tissues were obtained and processed for biochemical, light and electron microscopic studies from all animals in different study groups.

### *Biochemical study*

#### *1-Urea and creatinine*

Estimation of urea and creatinine plasma levels by utilizing an autoanalyzer (Hitach 912 Auto-Analyzer, Germany)<sup>[13]</sup>.

#### *2-Oxidant and Anti-oxidant markers*

For determination of oxidant and antioxidant enzymes, kidney tissues were dissected and then homogenized in potassium phosphate buffer solution (50Mm, Ph 7.5) via utilizing a potter Elvehjem homogenizer to allow 10 % homogenate. Homogenate were centrifuged, supernatant

was recovered, placed on ice, and immediately utilized for the estimation of MDA, SOD and CAT. SOD efficiency was estimated according to Nishikimi *et al.*<sup>[14]</sup> method. The principal of this method depends on SOD ability to prevent the power of phenazinemetosulphate-mediated to reduce the nitrobluetetrazolium. CAT activity was assayed according to Aebi<sup>[15]</sup> method and was estimated from the decomposition rate of H<sub>2</sub>O<sub>2</sub>. MDA as a marker for lipid peroxidation was measured colorimetrically in kidney homogenate according to the method of Ohkawa<sup>[16]</sup>.

### *Light microscopic study*

Right kidney specimens from all animal groups were fixed in formal saline. The specimens were processed for performing Paraffin sections, 7µm in thickness. Then sections were stained with hematoxylin and eosin (Hx&E) to illustrate the histological structure<sup>[17]</sup>.

For histochemical study, specimens from the renal cortex were fixed in cold acetone, then, processed and stained via calcium phosphate method in Gomori technique to determine the alkaline phosphatase enzyme. Histochemical activity of alkaline phosphatase in the proximal convoluted tubules has been detected. The reaction product was strongly marked at the apical surface and the basal part of the cells comprising the basal infoldings with their extended tips. The positive reaction was in the form of fine, uniform brown deposits<sup>[18]</sup>.

For immunohistochemical study of desmin (a podocyte injury marker): The primary monoclonal antibody was the mouse anti-desmin (Lab Vision Corp, Inc/Lab Vision, Fremont, USA). Negative control was performed via replacing the primary antibody with buffer alone. Leiomyoma was used as a positive control. The positive reaction was cytoplasmic brown color<sup>[19]</sup>. Counterstaining was performed using Mayer's hematoxylin.

For immunohistochemical study of BAX (a marker of apoptosis): The primary monoclonal antibody was the mouse anti-Bax (Ab-14 Golden, Lab Vision Clone B-9; Santa Cruz Biotechnology Inc., USA). Hodgkin's lymphoma was used as positive control. The positive reaction was cytoplasmic brown color<sup>[20]</sup>. Counterstaining was performed using Mayer's hematoxylin.

For immunohistochemical study of anti-proliferating cell nuclear antigen (PCNA): The primary monoclonal antibody was the mouse anti-PCNA (Santa Cruz Biotechnology Inc., USA). PCNA is used as the most reliable immunohistochemical marker for evaluating cell proliferation. Lymph node was used as a positive control. Nuclear staining with brown color was considered as a positive reaction<sup>[21]</sup>.

### *Transmission electron microscopic study*

Small pieces of the cortex of left kidneys from all animal groups were rapidly fixed in 3% glutaraldehyde solution and processed for examination, using a Jeol electron microscope. TEM processing and examination were carried out at the E.M Center, faculty of science, Alexandria University<sup>[22]</sup>.

### Morphometrical study

The renal corpuscles and proximal convoluted tubules diameters were measured in Hx&E stained sections. While, the area percentages of desmin, bax and PCNA expression were measured in immunostained sections, using the objective lens of magnification X40. From each animal 10 non overlapping microscopic fields were used. This was performed using the interactive measuring menu of image analyzer (LeciaQwin 500 image analyzer computer system, England) in anatomy department, faculty of medicine, Menoufia University.

The glomerular basement membrane (GBM) thickness was measured in three serial electron microscopic sections of three rats in different groups (five fields in each section) via utilizing image analyzer software at the electron microscope unit.

### Statistical analysis

The biochemical and morphometric results were analyzed and compared by student's t-test. P-value was utilized to test the significant change in the experimental groups in each parameter in comparison with the control group. Then, the collected data were tabulated as mean  $\pm$  SD and analyzed utilizing statistical package for the Social Science Software (SPSS)(version 17 on IBM compatible computer; SPSS Inc., Chicago, Illinois, USA). P value was set at 0.05,  $P > 0.05$  non-significant,  $P \text{ value} < 0.05$  significant<sup>[23]</sup>.

## RESULTS

### Biochemical results

#### 1-Kidney function tests (Urea and creatinine)

As shown in (Table 1), group II (CoQ10 treated group) revealed a non-significant changes in plasma levels of urea and creatinine ( $P > 0.05$ ) in comparison with the control animals. Group III (GA3 treated group) exhibited a highly significant increase in plasma levels of urea and creatinine ( $P < 0.001$ ) in comparison with the animals of control group. Moreover, group IV (CoQ10 and GA3 treated group) exhibited a non-significant ( $P > 0.05$ ) changes in the mean values of plasma levels of urea and creatinine when compared with the control animals. While revealed a highly significant decrease ( $P < 0.001$ ) in serum urea and creatinine levels in comparison with GA3 treated rats (Histograms 1a,1b).

#### 2-Oxidant and Anti-oxidant markers

As shown in (Table 2), group II (CoQ10 treated group) demonstrated a non-significant changes in the levels of MDA (lipid peroxidation marker), SOD and CAT (antioxidant enzymes) ( $P > 0.05$ ) in comparison with control animals. Group III (GA3 treated group) exhibited a significant increase in the level of MDA ( $P < 0.05$ ) and a highly significant decrease in the level of SOD and CAT ( $P < 0.001$ ) in comparison with the animals of control group. Moreover, group IV (CoQ10 and GA3 treated group) exhibited a non-significant changes in the mean values of MDA, SOD & CAT ( $P > 0.05$ ) in comparison with the control

animals, while revealed a highly significant increase in the level of antioxidant enzymes in comparison with GA3 treated group ( $P < 0.001$ ) (Histograms 2a,2b)

### Light microscopic results

Hx&E stained sections of the renal cortex of groups I&II (control & CoQ10 treated groups) were the same and revealed the renal corpuscle which contained glomerular capillaries and surrounded with parietal and visceral layers of bowman's capsule, the two layers were separated by bowman's space. The parietal layer was formed of simple squamous epithelium. Also, Proximal convoluted tubules (PCT) lined with pyramidal cells with deeply acidophilic cytoplasm and vesicular nuclei were observed. Distal convoluted tubules (DCT) showed wide lumen and its lining cells had apical nuclei and less acidophilic cytoplasm (Figures 1,2).

Sections of the renal cortex of group III (GA3 treated group) exhibited glomerular and tubular changes. Renal corpuscle appeared with marked atrophy of the glomerulus with widening of bowman's space (Figure 3). Also, congestion of the glomerular capillaries (Figure 4) was observed. Some renal corpuscles appeared with obliteration of bowman's space. others revealed marked cellular infiltration (Figure 7). Some renal tubular cells revealed cytoplasmic vacuoles and small pyknotic nuclei (Figures 3,4,5), others showed rarefaction (Figures 3,4). Some exfoliated cells and nuclei in the lumen were also present, whereas other tubules revealed necrotic epithelium and marked tubular dilatation (Figure 4). Hyalinization of lining cells and lumen with flattened nuclei of some tubular cells were noticed (Figures 5,6). The interstitium of the renal cortex revealed heavy cellular infiltration (Figure 6) and blood vessels congestion (Figure 7).

Sections of the renal cortex of group IV (CoQ10 and GA3 treated group) displayed nearly normal appearance of glomeruli, proximal and distal convoluted tubules (Figure 8).

Regarding to alkaline phosphatase enzyme reaction of groups I&II (control & CoQ10 treated groups) displayed strong positive reaction at the apical surfaces and basal parts of the proximal convoluted tubular cells (Figures 9,10). While examination of group III (GA3 treated group) exhibited marked decrease in alkaline phosphatase reaction at the apical surfaces and basal parts of the proximal convoluted tubular cells in comparison with the control animals (Figure 11). Section of the renal cortex of group IV (CoQ10 and GA3 treated group) displayed increased reaction compared with group III (Figure 12).

Regarding Desmin immune-marker expression, kidney tissue obtained from groups I&II (control & CoQ10 treated groups) showed negative expression of desmin in the glomerular epithelial cells (Figures 13,14). Group III (GA3 treated group) revealed strong positive cytoplasmic desmin immunostaining in the glomerular epithelial cells (Figure 15). While group IV (CoQ10 and GA3 treated group) revealed a moderate cytoplasmic desmin expression (Figure 16).

Regarding Bax immune-marker expression, kidney tissue of groups I&II (control & CoQ10 treated groups) showed negative immunoreactivity for Bax in the renal tubular cells and glomeruli (Figures 17,18). Group III (GA3 treated group) revealed strong positive cytoplasmic Bax immunoreaction in the renal tubular cells and glomeruli (Figure 19). Sections of the renal cortex of group IV (CoQ10 and GA3 treated group) displayed weak cytoplasmic Bax immunoreaction in some renal tubular cells and glomeruli (Figure 20).

Regarding PCNA immune-marker expression, kidney tissue obtained from groups I&II (control & CoQ10 treated groups) revealed a few number of positive PCNA immunoreaction in renal tubular cells (Figures 21,22). Group III (GA3 treated group) revealed increase positive PCNA immune reaction in renal tubular cells (Figure 23). While group IV (CoQ10 and GA3 treated group) revealed decrease positive PCNA immunoreaction (Figure 24).

### Transmission electron microscopic results

Ultra-thin sections of the renal cortex of control animals (groups I&II) exhibited a renal corpuscle with a glomerular blood capillary lined by fenestrated endothelium and surrounded with a podocyte which had rounded euchromatic nucleus and from the cell body arise primary processes and multiple secondary processes (foot processes) which rest on a regular basement membrane (Figures 25,28). The proximal convoluted tubular cell exhibited rounded euchromatic nucleus with prominent nucleolus, long apical microvilli, rough endoplasmic reticulum, Golgi apparatus and multiple basal elongated mitochondria in the cytoplasm (Figures 26,29). The distal convoluted tubular cells had rounded euchromatic nucleus, few apical microvilli and mitochondria in the cytoplasm. There was a tight junction of the plasmalemma of adjoining cells (Figure 27). An electron microscopic examination of Group III (GA3 treated group) revealed a glomerular capillary with glomerular basement membrane thickening. The podocyte had nucleus with irregular outline and dilated cisternae of rough endoplasmic reticulum. Fused foot processes and apparent thinning of the primary process were seen (Figure 30). The proximal convoluted tubular cell revealed euchromatic nucleus with widened perinuclear space (Figure 31), destruction of apical microvilli was observed, its cytoplasm contained hypertrophied mitochondria, vacuoles and numerous lysosomes (Figure 32). The distal convoluted tubular cell appeared with apoptotic nucleus, distorted apical membrane and disorganization of basal infoldings. Its cytoplasm appeared vacuolated, containing irregularly arranged mitochondria with destroyed cristae in some of them (Figure 33). An electron microscopic examination of the Group IV (CoQ10 and GA3 treated group) revealed glomerular capillaries with minimal focal glomerular basement membrane thickening. The podocytes had indented nucleus, cytoplasmic vacuoles, primary processes and secondary processes (Figure 34). The proximal convoluted tubular cell revealed rounded euchromatic nucleus, multiple mitochondria and luminal microvilli (Figure 35). The distal

tubular cells displayed apical euchromatic rounded nuclei and basally located numerous mitochondria. The tubular lumen was observed (Figure 36).

### Morphometric results

Data in (Table 3) demonstrated that group III (GA3 group) exhibited a highly significant increase in the glomerular basement membrane thickness in comparison with the control rats ( $P<0.001$ ), while group IV (CoQ10 and GA3 treated group) displayed a significant increase in comparison with the control animals ( $P<0.05$ ) and a highly significant changes ( $P<0.001$ ) in comparison with GA3 treated rats (group III) (Histogram 3a).

In addition, group III (GA3 group) exhibited a highly significant decrease in the renal corpuscle diameter ( $P<0.001$ ) and a highly significant increase in the diameter of renal tubules ( $P<0.001$ ) in comparison with the control animals. However, CoQ10 administration greatly improved the morphometric results concerning the renal corpuscle and renal tubule diameters.

As group IV (CoQ10 and GA3 treated group) revealed a non-significant change in comparison with the control animals and a highly significant change when compared with GA3 treated animals (Histogram 3b).

Data in (Table 4) showed that group III (GA3) exhibited a highly significant increase ( $P<0.001$ ) in the mean area % of desmin, Bax and PCNA immunoreactions in the kidney tissue of animals when compared with the control group. However, group IV (CoQ10 and GA3 treated group) showed a highly significant decrease ( $P<0.001$ ) in comparison with GA3 treated group (Histogram 4).

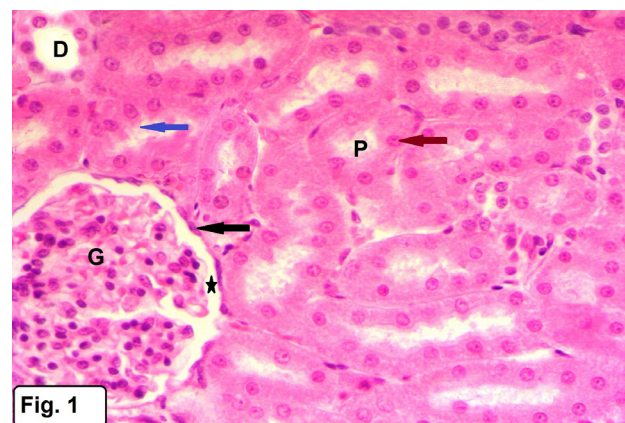


**Fig. 1:** A photomicrograph of the renal cortex of control group (group I) showing a renal corpuscle with a glomerulus (G), surrounded with parietal and visceral layers of Bowman's capsule, they are separated by Bowman's space (star), the parietal layer is formed of simple squamous epithelium (black arrow). Proximal convoluted tubules (P) are lined with pyramidal cells which have brush border (blue arrow), deeply acidophilic cytoplasm and vesicular nuclei (red arrow). Distal convoluted tubules (D) shows wide lumen and its lining cells have apical nuclei and less acidophilic cytoplasm.



**Fig. 2:** A photomicrograph of the renal cortex of CoQ10 treated group (group II) showing a renal corpuscle with a glomerulus (G), surrounded by parietal and visceral layers of Bowman's capsule, they are separated by Bowman's space (star). Proximal convoluted tubules (P) and distal convoluted tubules (D) are seen. Hx&E X200

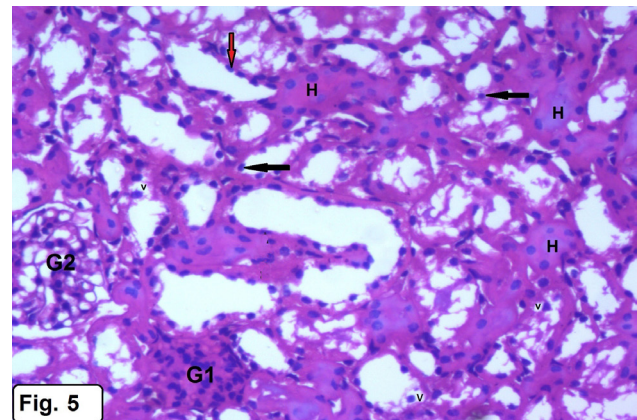


**Fig. 5:** A photomicrograph of the renal cortex of GA3 treated group (group III) showing renal tubular cells with cytoplasmic vacuoles (v) and pyknotic nuclei (black arrows). Hyalinization of lining cells and lumen of some renal tubules (H) is seen. Some lining epithelial tubular cells are flattened (red arrow). Notice, renal corpuscle (G1) appears with obliteration of Bowman's space. Other renal corpuscle (G2) appears normal. Hx&E X200

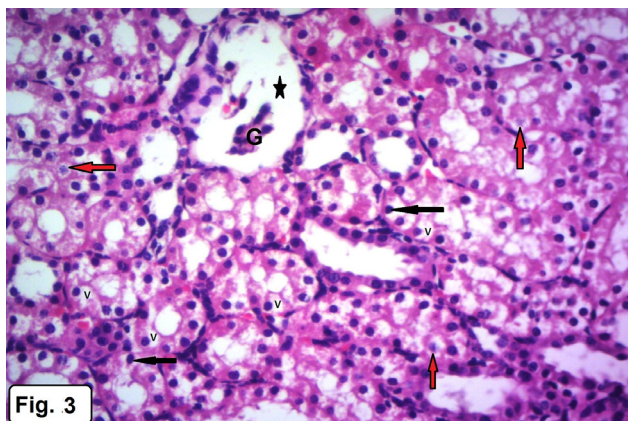


**Fig. 3:** A photomicrograph of the renal cortex of GA3 treated group (group III) showing a renal corpuscle with marked atrophy of the glomerulus (G) and Bowman's space widening (star). The renal tubular cells show cytoplasmic vacuoles (V) and pyknotic nuclei (black arrows), others show rarefaction (red arrows). Hx&E X200

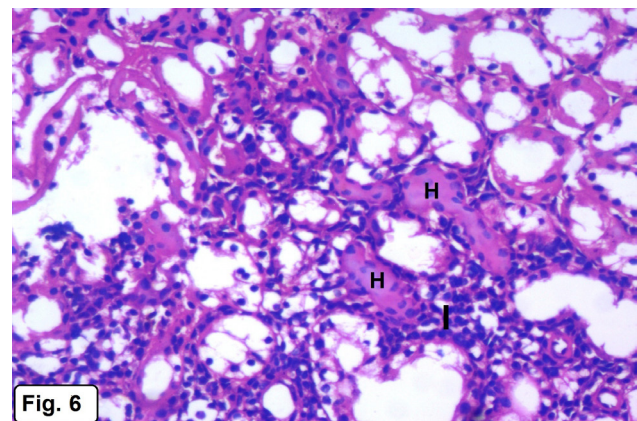


**Fig. 6:** A photomicrograph of the renal cortex of GA3 treated group (group III) showing heavy interstitial cellular infiltration (I) and hyalinization of some renal tubules (H). Hx&E X 200

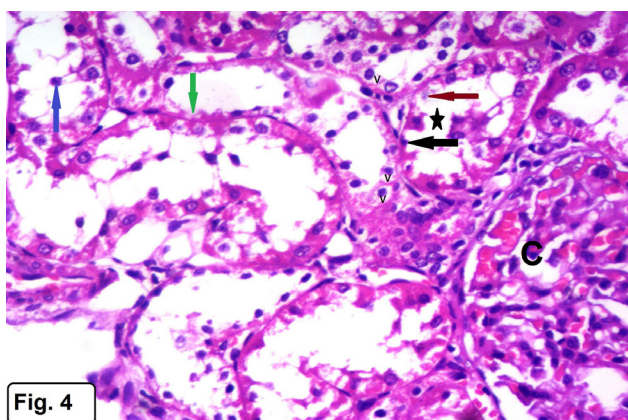


**Fig. 4:** A photomicrograph of the renal cortex of GA3 treated group (group III) showing glomerular capillaries congestion (C), the renal tubular cells appear with vacuolation of their cytoplasm (V) and pyknotic nuclei (black arrow), rarefaction of some tubular cells are observed (red arrow). Some exfoliated cells and nuclei are shed in lumen (blue arrow). Notice, necrosis of some tubular cells (green arrow) and marked tubular dilatation (star). Hx&E X200

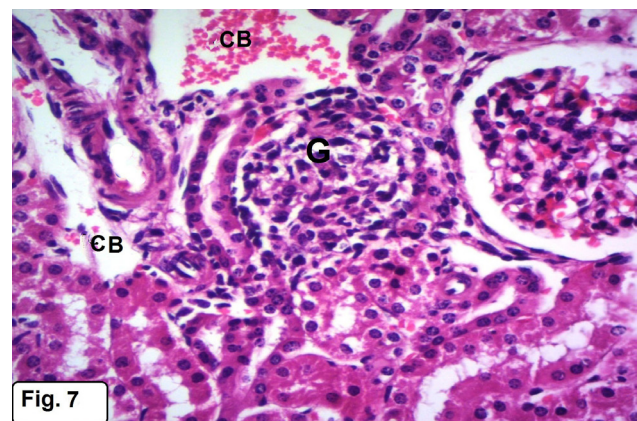


**Fig. 7:** A photomicrograph of the renal cortex of GA3 group (group III) showing a renal corpuscle (G) with heavy cellular infiltration and obliteration of the Bowman's space. Notice, congestion of the blood vessel (CB). Hx&E X200

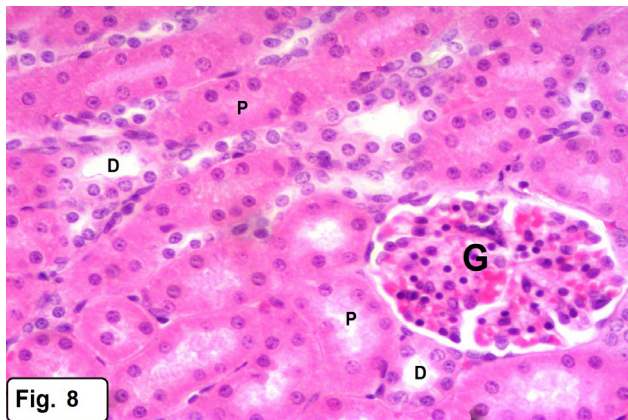


**Fig. 8**

**Fig. 8:** A photomicrograph of the renal cortex of CoQ10 and GA3 treated group (group IV) showing nearly normal appearance of the glomerulus (G), proximal (P) and distal (D) convoluted tubules. Hx&E X200

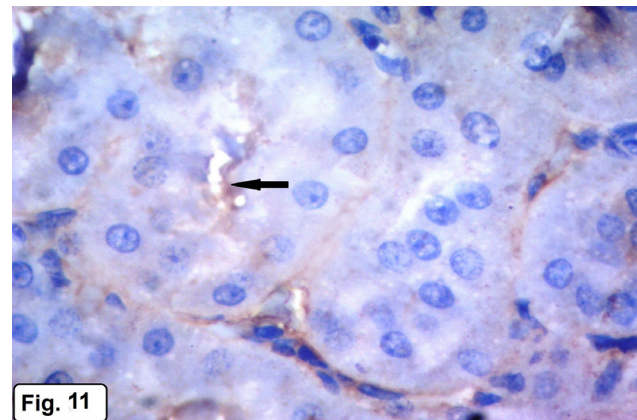


**Fig. 11**

**Fig. 11:** A photomicrograph of the renal cortex of GA3 group (group III) showing marked decrease in alkaline phosphatase positive reaction at the apical surface and basal parts of the proximal convoluted tubular cells (arrow). Alk. phosphatase X400

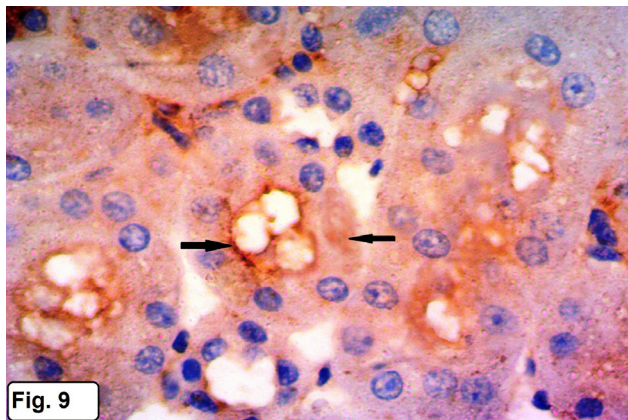


**Fig. 9**

**Fig. 9:** A photomicrograph of the renal cortex of control group (group I) showing strong positive reaction for alkaline phosphatase at the apical surfaces and basal parts of the proximal convoluted tubular cells (arrows). Alk. phosphatase X400

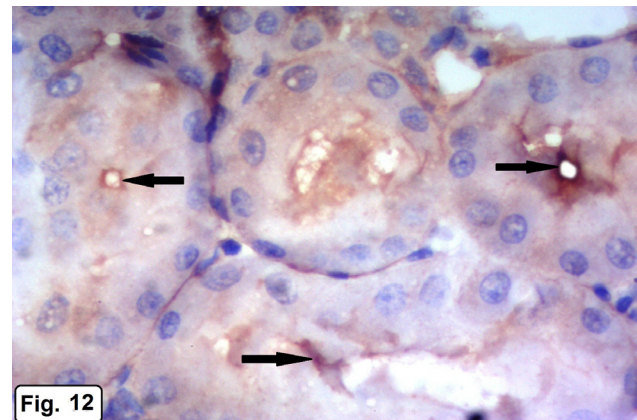


**Fig. 12**

**Fig. 12:** A photomicrograph of the renal cortex of CoQ10 and GA3 treated group (group IV) showing increased positive reaction for alkaline phosphatase (arrows) compared with group III. Alk. phosphatase X400

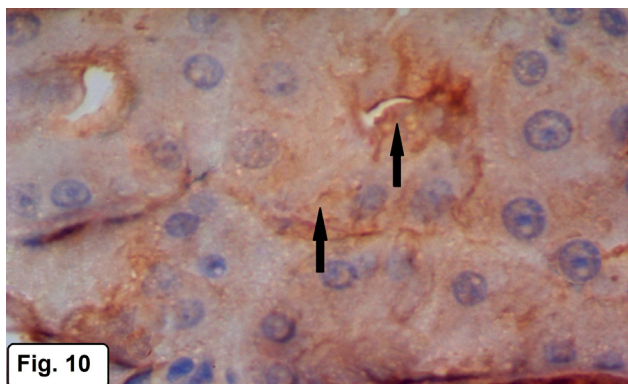


**Fig. 10**

**Fig. 10:** A photomicrograph of the renal cortex of CoQ10 treated group (group II) showing strong positive reaction for alkaline phosphatase at the apical surfaces and basal parts of the proximal convoluted tubular cells (arrows). Alk. phosphatase X400

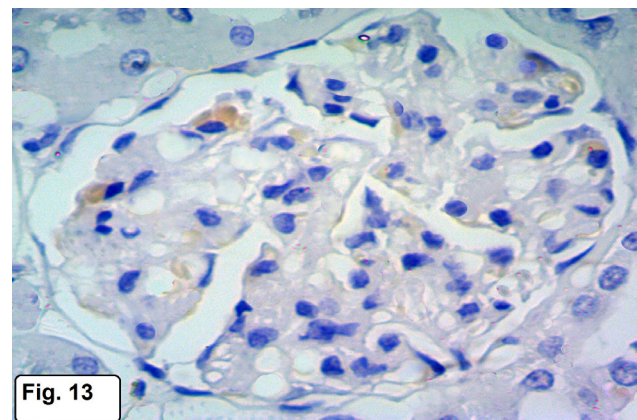


**Fig. 13**

**Fig. 13:** A photomicrograph of the renal cortex of control group (group I) showing negative cytoplasmic desmin immunostaining in the glomerular epithelial cells. Desmin X 400

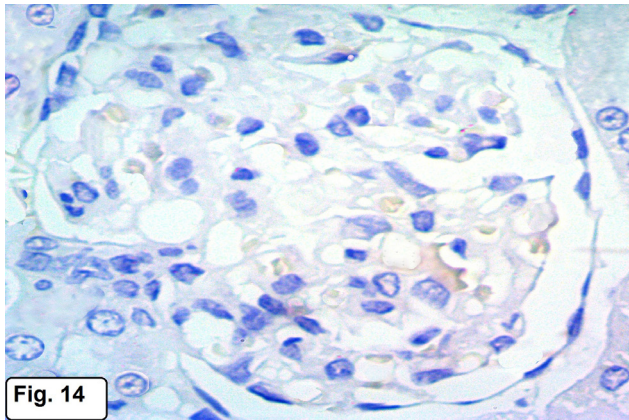


**Fig. 14**

**Fig. 14:** A photomicrograph of the renal cortex of CoQ10 treated group (group II) showing negative cytoplasmic desmin immunostaining in the glomerular epithelial cells. Desmin X 400

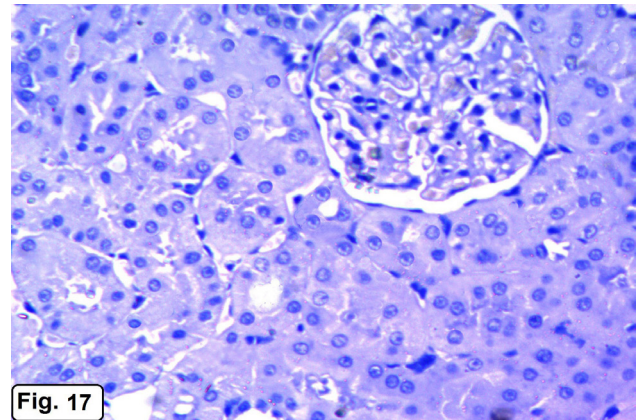


**Fig. 17**

**Fig. 17:** A photomicrograph of the renal cortex of control group (group I) showing negative cytoplasmic immunoreactivity for Bax in the renal tubular cells and glomeruli. Bax X200

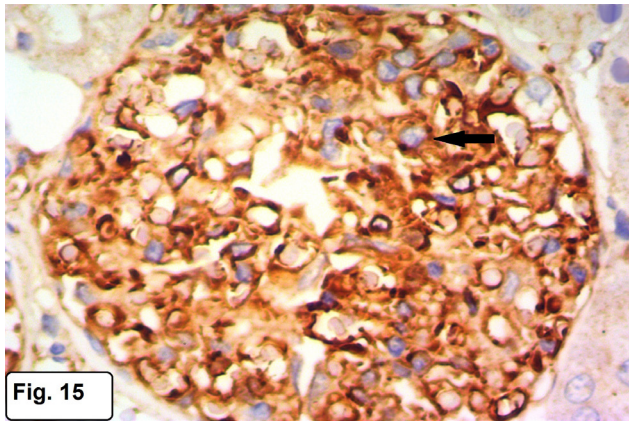


**Fig. 15**

**Fig. 15:** A photomicrograph of the renal cortex of GA3 treated group (group III) showing strong positive cytoplasmic desmin immunostaining in the glomerular epithelial cells (arrow). Desmin X 400

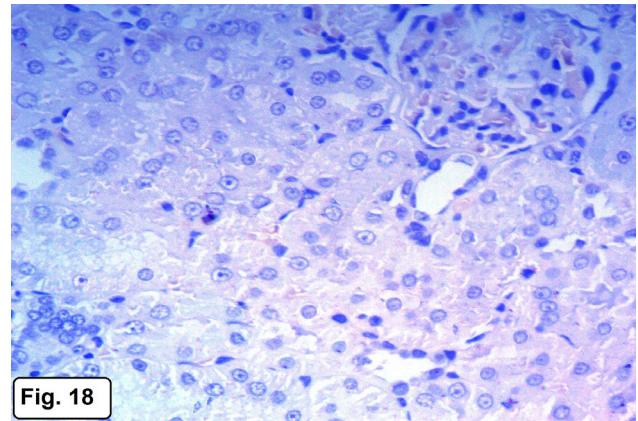


**Fig. 18**

**Fig. 18:** A photomicrograph of the renal cortex of CoQ10 treated group (group II) showing negative cytoplasmic immunoreactivity for Bax in the renal tubular cells and glomeruli. Bax X200

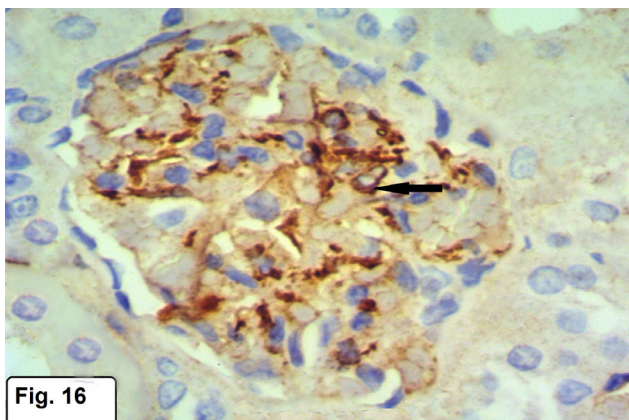


**Fig. 16**

**Fig. 16:** A photomicrograph of the renal cortex of CoQ10 and GA3 treated group (group IV) showing moderate cytoplasmic desmin immunostaining in the glomerular epithelial cells (arrow). Desmin X 400

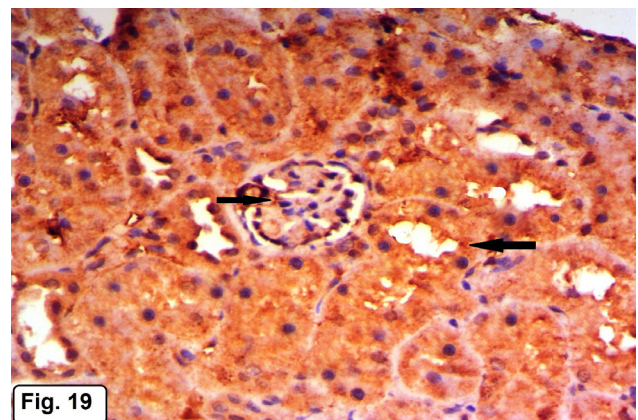


**Fig. 19**

**Fig. 19:** A photomicrograph of the renal cortex of GA3 treated group (group III) showing strong positive cytoplasmic Bax immunoreactivity (brown granules) in the glomeruli and renal tubular cells (arrows). Bax X200

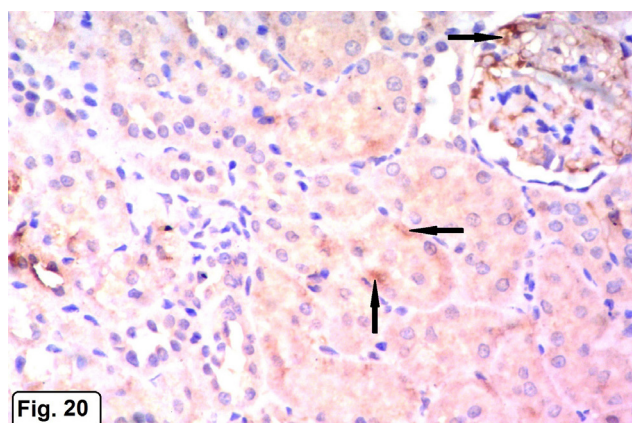


**Fig. 20**

**Fig. 20:** A photomicrograph of the renal cortex of CoQ10 and GA3 treated group (group IV) showing weak cytoplasmic Bax immunoreactivity in some renal tubular cells and glomeruli (arrows). Bax X200

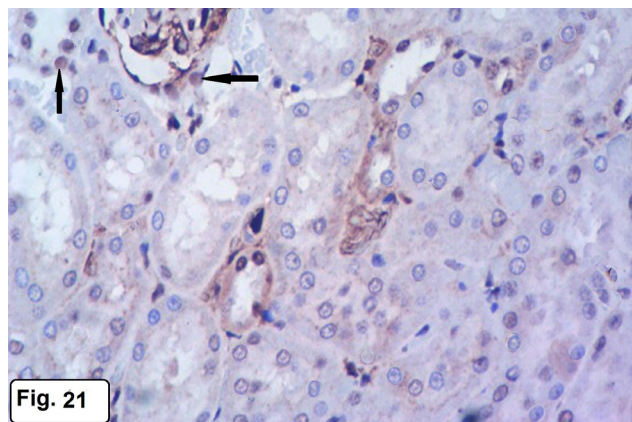


**Fig. 21**

**Fig. 21:** A photomicrograph of the renal cortex of control group (group I) showing a few number of positive PCNA immunoreactivity in renal tubular cells (arrows). PCNA X200

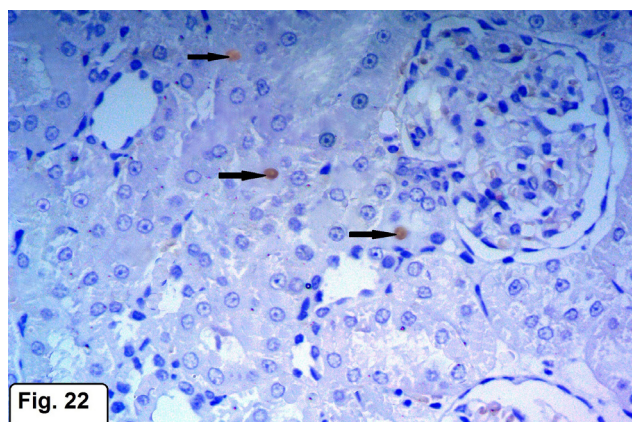


**Fig. 22**

**Fig. 22:** A photomicrograph of the renal cortex of CoQ10 treated group (group II) showing a few number of positive PCNA immunoreactivity in renal tubular cells (arrows). PCNA X200

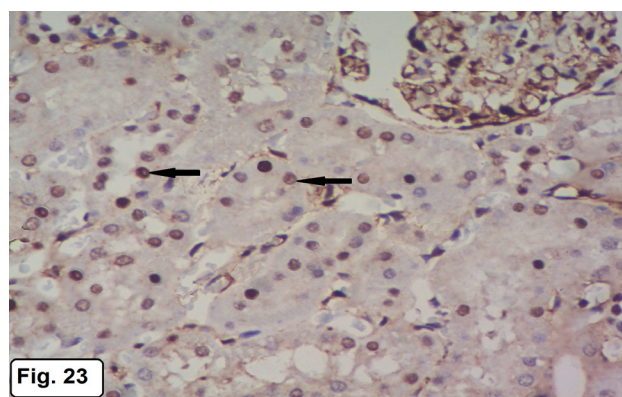


**Fig. 23**

**Fig. 23:** A photomicrograph of the renal cortex of GA3 treated group (group III) showing an increase in the number of positive nuclear PCNA immunoreactivity in renal tubular cells (arrows) PCNA X200

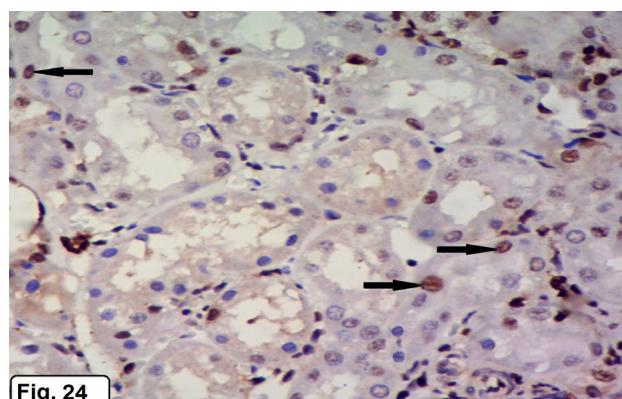


**Fig. 24**

**Fig. 24:** A photomicrograph of the renal cortex of CoQ10 and GA3 treated group (group IV) showing decreased positive nuclear PCNA immunoreactivity in renal tubular cells (arrows). PCNA X200

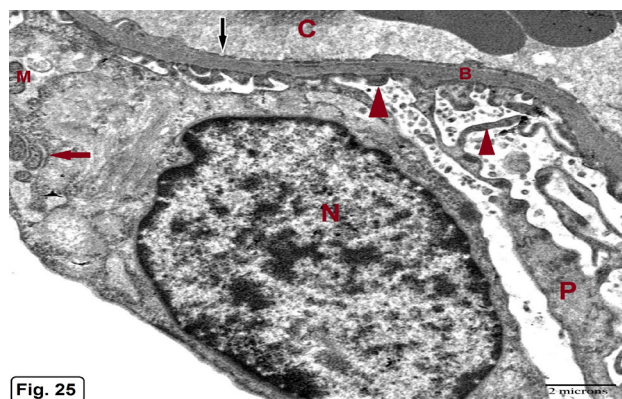


**Fig. 25**

**Fig. 25:** An electron micrograph of a renal corpuscle of control group (group I) showing a glomerular blood capillary (C) lined by fenestrated endothelium (black arrow) and surrounded by podocyte with rounded euchromatic nucleus (N), rough endoplasmic reticulum cisternae (red arrow) and mitochondria (M). From the cell body arises primary processes (P) and multiple secondary processes (arrowheads) which rest on regular basement membrane (B). X15000



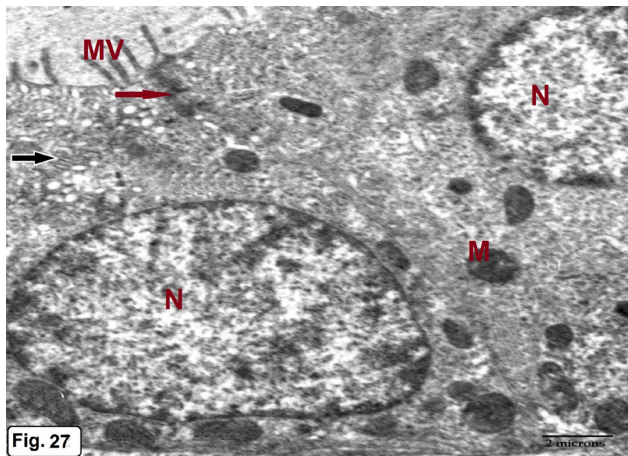


Fig. 27

Fig. 27: An electron micrograph of the distal convoluted tubular cells of a control group (group I) showing euchromatic rounded nucleus (N), few apical microvilli (MV), rough endoplasmic reticulum cisternae (black arrow) and mitochondria (M). Notice, tight junction of the plasmalemma of adjoining cells (red arrow). X 15000

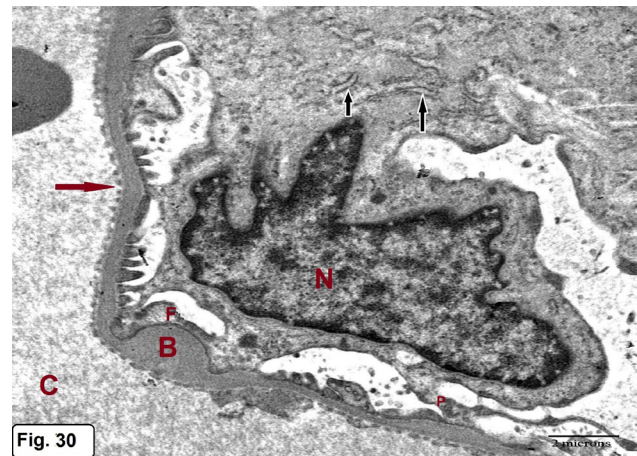


Fig. 30

Fig. 30: An electron micrograph of a renal corpuscle of GA3 treated group (group III) showing a glomerular capillary (C) with irregular thickening of the glomerular basement membrane (B). The podocyte has nucleus with irregular outline (N), dilated cisternae of rough endoplasmic reticulum (black arrows) and fused foot processes (F). Notice, apparent thinning of the primary process (P). X 15000

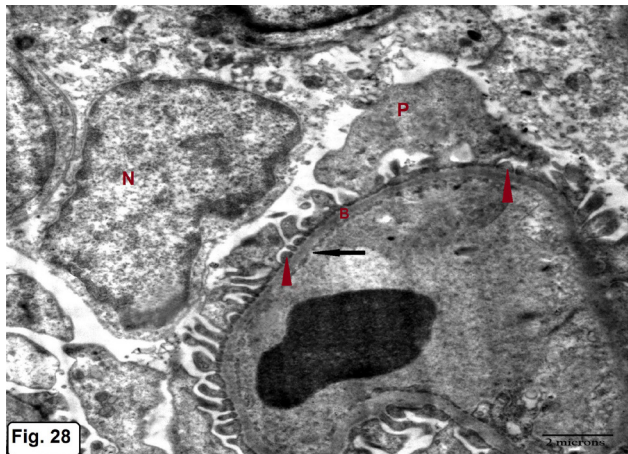


Fig. 28

Fig. 28: An electron micrograph of a renal corpuscle of CoQ10 treated group (group II) showing a glomerular blood capillary (C) lined by fenestrated endothelium (black arrow) and surrounded by podocyte with euchromatic nucleus (N). From the cell body arises primary processes (P) and multiple secondary processes (arrowheads) which rest on regular basement membrane (B). X15000

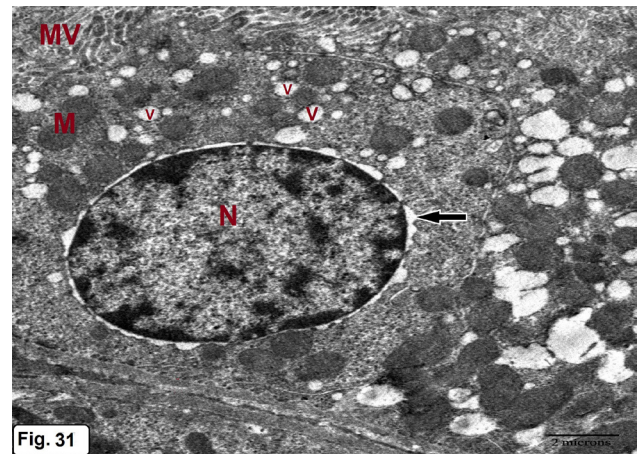


Fig. 31

Fig. 31: An electron micrograph of a proximal tubular cell of GA3 treated group (group III) showing rounded euchromatic nucleus (N) with widened perinuclear space (black arrow), multiple mitochondria (M) and cytoplasmic vacuoles (V). Notice, some apical microvilli (MV). X15000

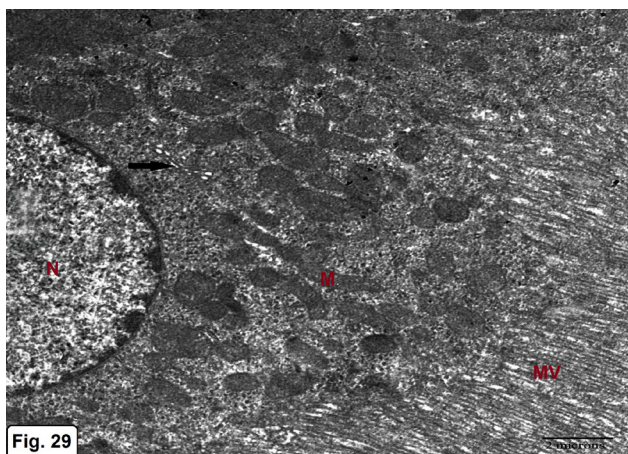


Fig. 29

Fig. 29: An electron micrograph of the proximal convoluted tubular cell of CoQ10 treated group (group II) showing euchromatic rounded nucleus (N), long apical closely packed microvilli (MV), numerous mitochondria (M) and golgi apparatus (arrow) in the cytoplasm. X 15000

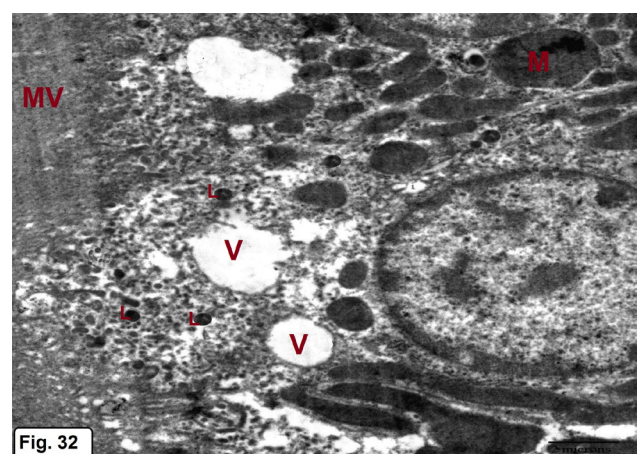
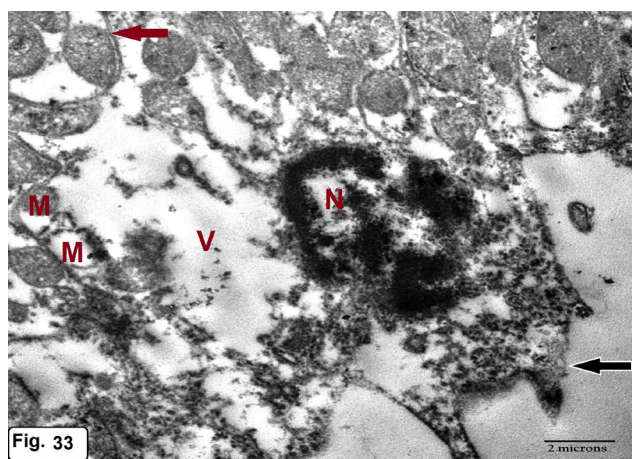
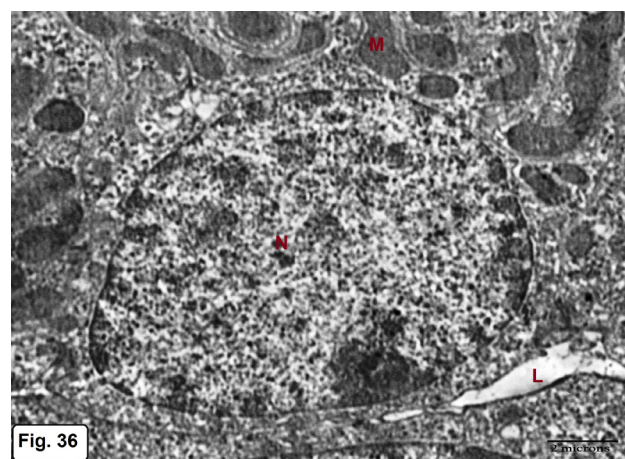


Fig. 32

Fig. 32: An electron micrograph of the proximal convoluted tubular cells of a GA3 treated group (group III) showing destruction of apical microvilli (MV), hypertrophied mitochondria (M), cytoplasmic vacuoles (V) and numerous lysosomes (L). X 15000



**Fig. 33:** An electron micrograph of a distal tubular cell of GA3 treated group (group III) showing apoptotic nucleus (N), distorted apical membrane (black arrow) with disorganization of basal infoldings (red arrow). The cytoplasm is vacuolated (V) and contains irregularly arranged mitochondria with destroyed cristae in some of them (M). X 15000



**Fig. 36:** An electron micrograph of the distal tubular cells of CoQ10 and GA3 treated group (group IV) showing apical rounded euchromatic nuclei (N), basally located multiple mitochondria (M). Notice, the tubular lumen (L). X 15000

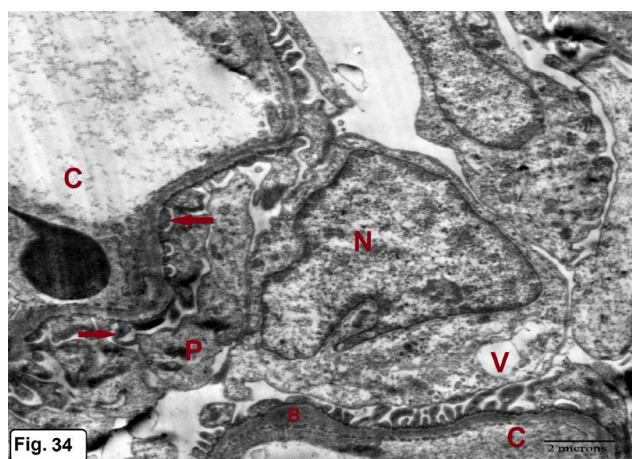


**Fig. 34:** An electron micrograph of a renal corpuscle of CoQ10 and GA3 treated group (group IV) showing glomerular capillaries (C) with minimal focal thickening of the glomerular basement membrane (B). The podocyte appears with indented nucleus (N), cytoplasmic vacuole (V), primary processes (P) and secondary processes (arrows). X15000

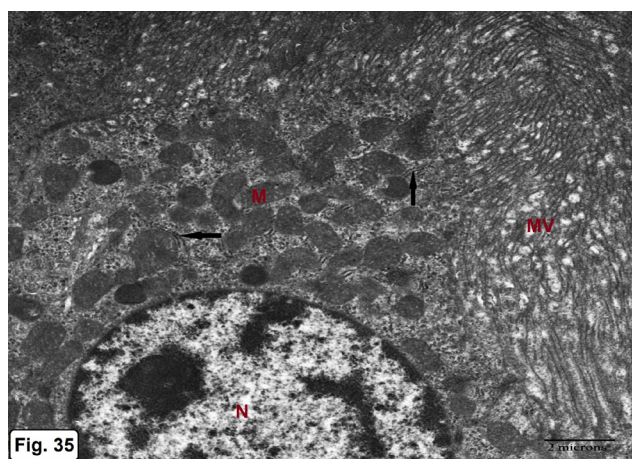


**Fig. 35:** An electron micrograph of the proximal tubular cell of CoQ10 and GA3 treated group (group IV) showing rounded euchromatic nucleus (N), multiple mitochondria (M), rough endoplasmic cisternae (arrows) and luminal microvilli (MV). X15000

**Table 1:** Mean plasma levels of urea and creatinine in different experimental groups

	Group I	Group II	Group III	Group IV	
urea (mg/dl)	27.2±0.7	26.8±0.6	75.4±1	28±2	P1=.218
					P2=.000
					P3=.219
					P4=.000
creatinine (mg/dl)	0.4±0.1	0.4±0.1	1.3±0.5	0.4±0.3	P1=.681
					P2=.000
					P3=.383
					P4=.000

M= the mean value. SD= the standard deviation.

**P1** Comparison was done between group II (CoQ10 treated group) and control group.

**P2** Comparison was done between group III (GA3 treated group) and control group.

**P3** Comparison was done between group IV (CoQ10 and GA3 treated group) and control group.

**P4** Comparison was done between group IV (CoQ10 and GA3 treated group) and group III (GA3 treated group)

**Table 2:** Mean values of MDA, SOD and CAT in renal tissue of all groups

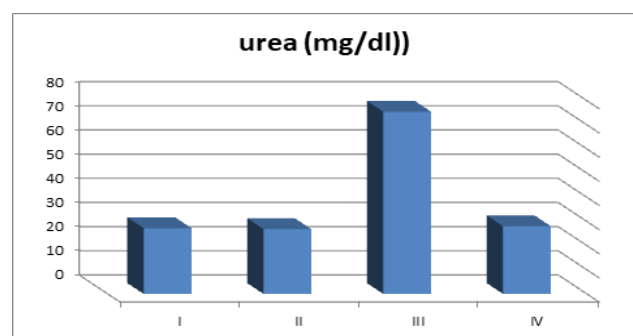
	Group I	Group II	Group III	Group IV	
MDA (nmol/mg)	16±0.8	15.7±1.1	27.8±13.2	19.6±5.8	P1=.473
					P2=.011
					P3=.065
					P4=.08
SOD (u/mg)	215.6±1.9	214.7±1.9	158.3±5.6	204.2±18.1	P1=.294
					P2=.000
					P3=.062
					P4=.000
CAT (u/mg)	526±3.7	528.1±2.1	314.7±4	513.5±22.4	P1=.283
					P2=.000
					P3=.085
					P4=.000

**Table 3:** Means values of the glomerular basement membrane thickness, diameter of the renal corpuscles and proximal convoluted tubules in different experimental groups

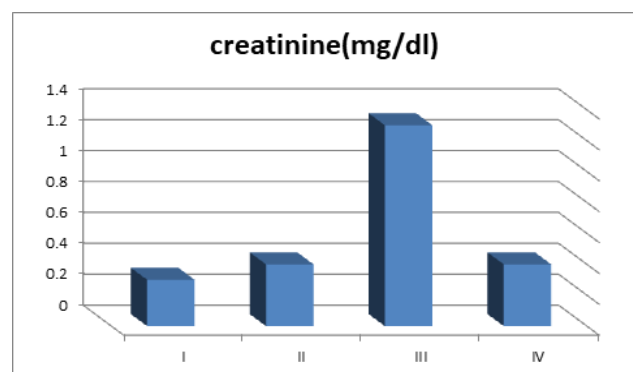
	Group I	Group II	Group III	Group IV	
GBM (nm)	164.7±5.1	167.8±6.8	401.6±11.9	213.5±5.3	P1=.268 P2=.000 P3=.01 P4=.000
Renal corpuscle (µm)	126.8±2.4	127.1±1.3	86.4±2.5	121±9.1	P1=.718 P2=.000 P3=.068 P4=.000
Tubular diameter (µm)	45.3±1	43.6±3.7	73.7±2.5	42.6±4.8	P1=.173 P2=.000 P3=.100 P4=.000

**Table 4:** percentages of desmin, Bax and PCNA expression in different experimental groups

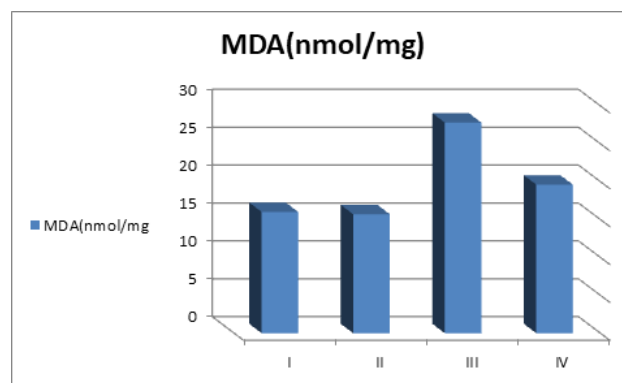
	Group I Mean±SD	Group II Mean±SD	Group III Mean±SD	Group IV Mean±SD	
Desmin (%)	0.5±0.2	0.6±0.2	19.6±1.6	3.6±3.9	P1=0.079 P2=0.000 P3=0.021 P4=0.000
Bax (%)	2.8±0.5	2.4±0.3	26.4±1.7	5.9±3.1	P1=0.06 P2=0.000 P3=0.006 P4=0.000
PCNA (%)	0.3±0.2	0.4±0.2	1.7±0.3	0.6±0.3	P1=0.376 P2=0.000 P3=0.019 P4=0.000



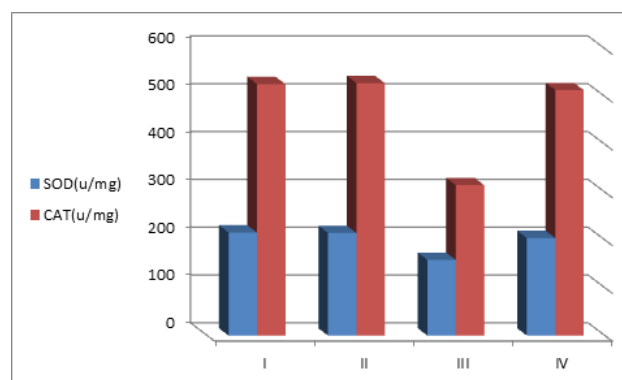
**Histogram 1a:** Mean plasma urea concentrations in different groups



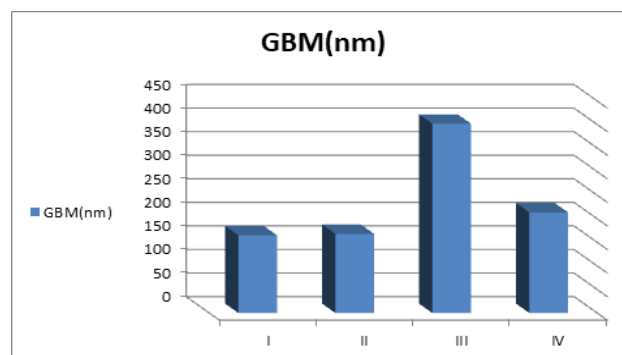
**Histogram 1b:** Mean plasma creatinine concentrations in different groups



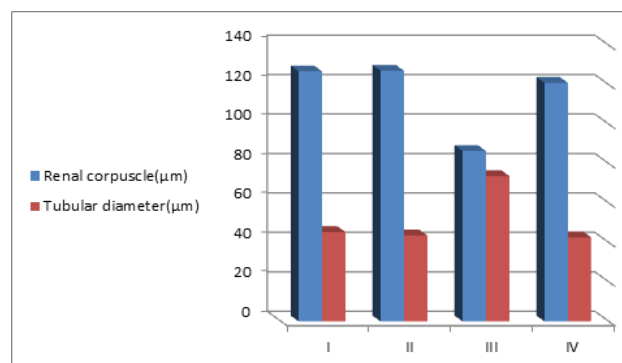
**Histogram 2a:** Mean values of MDA in renal tissue in all groups



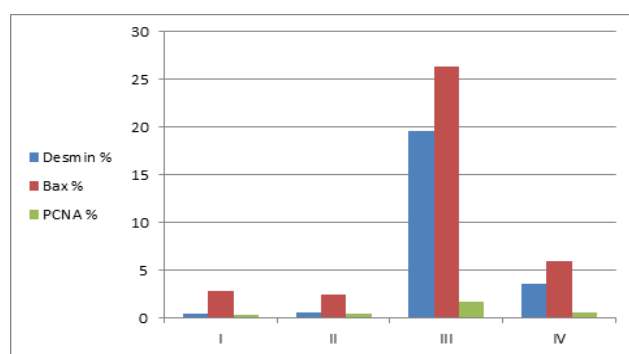
**Histogram 2b:** Mean values of SOD and CAT in renal tissue in all groups



**Histogram 3a:** Mean values of the glomerular basement thickness in all groups



**Histogram 3b:** Mean values of the renal corpuscles and proximal convoluted tubules diameter in all groups



**Histogram 4:** Mean desmin, Bax and PCNA immunoreactions in all groups

## DISCUSSION

GA3 is one of the plant growth regulators commonly used in agriculture and classified by WHO as pesticides [1]. Little is about its hazardous effect on human health<sup>[24]</sup>. The most common target organs for GA3 toxicity is the kidney as it concentrates toxins and metabolites<sup>[25]</sup>. Kidney is an essential organ in maintaining homeostasis and regulation of extracellular environment by detoxication and excretion of toxic metabolites<sup>[26]</sup>, so this work was designed to reveal histological, histochemical and immunohistochemical effects of GA3 on the renal cortex structure and the potential protective role of CoQ10.

The light microscopic results of GA3 treated animals showed atrophy of some renal corpuscles with obliteration of bowman's space, the renal tubules revealed marked dilatation with vacuolation and necrosis of their lining cells, some renal tubules showed hyalinization with obliteration of their lumen, heavy cellular infiltration and congestion of blood vessels were also seen.

These changes were in agreement with<sup>[4]</sup> who reported the same changes on kidney with GA3<sup>[27]</sup>. These histopathological changes may be due to participation of kidney in elimination of GA3 which was in acceptance with<sup>[28]</sup>. Atrophic corpuscles with wide bowman's spaces may be due to periglomerular fibrosis and thickened glomerular basement membrane leading to disturbance in glomerular out flow and cystic changes in bowman's space<sup>[29]</sup>.

Cytoplasmic vacuolation of the renal tubular cells caused by intracellular water accumulation due to increased permeability of cell membranes. Heavy cellular infiltration and vascular congestion were observed in the current study may be explained as an injurious toxins defense mechanism<sup>[30]</sup>.

These findings were confirmed morphometrically by showing a marked decrease in the diameter of renal corpuscle and a marked increase in the diameter of renal tubules compared to the control animals.

The biochemical findings of GA3 treated animals detected in the current study was substantiated with the kidney histopathological changes. A significant increased plasma level of urea and creatinine were observed, indicating renal dysfunction, which was in harmony with<sup>[12]</sup>.

kidney injury and structural damage seen in GA3 treated results may be explained by cellular oxidative stress (OS) as our results revealed increase in MDA and decrease in antioxidant enzymes CAT and SOD parameters which was coinciding with<sup>[31]</sup> who explained kidney injury after GA3 exposure is due to an increase in MDA (end product of lipid peroxidation) with change in enzymatic antioxidant defense system with subsequent increase in reactive oxygen species (ROS).<sup>[32]</sup> found decrease in non enzymatic glutathione (GSH) antioxidant which might lead to increase in Reactive Oxygen Species (ROS). Release of ROS can cause cell dysfunction and finally, cell death by attacking DNA, lipids and thiols in proteins<sup>[33]</sup>.

Cellular degeneration and necrosis of the renal tubules and glomeruli may be due to apoptosis as GA3 treated group showed strong positive BAX immune reaction (proapoptotic protein). BAX induces apoptosis by the formation of ion channels in ER membranes to release  $Ca^{2+}$ <sup>[34]</sup>, formation of mitochondrial permeability transition pores leading to necrosis<sup>[35]</sup> and cytochrome C release with caspase 3,8 activation<sup>[36]</sup>, these BAX results is in parallel with<sup>[37]</sup> who revealed strong BAX reaction with renal injury due to hemorrhagic shock.

Reported<sup>[38]</sup> an increase in PCNA immunostain on liver and kidney with Ethephon intoxication (one of PGRs), this was in agreement with our results which showed strong reaction of PCNA on kidney with GA3, this may be explained by<sup>[30]</sup> who reported that GA3 increase mitotic division to promote growth of tissues and is considered a compensatory proliferating mechanism to compensate kidney damage manifested by apoptosis and strong BAX reaction<sup>[39]</sup>.

Our results revealed marked increase in desmin immunostain in renal corpuscles of GA3 treated group, that increase may be explained by podocyte injury as intermediate filament desmin is a sensitive marker for its injury. Its expression was upregulated in different glomerular diseases in which podocytes injuries were involved<sup>[40]</sup>. This is in accordance with<sup>[41]</sup> who reported desmin upregulation and increase in glomeruli of hypertensive nephropathy,<sup>[42]</sup> reported that transforming growth factor B1 (TGF B1) induced by glomerulosclerosis increase expression of desmin and capsase9 leading to apoptosis and<sup>[43]</sup> noticed increase in reaction with bisphenol nephrotoxicity. Our results revealed decrease in reaction with concomitant administration of CoQ10 which is in harmony with<sup>[44]</sup> who stated that decrease in desmin protein expression play important role in regulating injured podocyte

Our electron microscopic results of GA3 treated group revealed many histopathological changes which confirm light microscopic results as there was irregular thickening of the glomerular basement membrane which confirmed morphometrically, and this finding may be due to large surface area of glomerular capillaries rendering them more susceptible to damage by circulating toxins and immune complex<sup>[45]</sup>. Tubular lining cells showed vacuoles, damaged mitochondria, numerous lysosomes and destruction of

apical microvilli, these changes may be due to their necrosis secondary to contact with toxins<sup>[46]</sup>, dilated RER indicated increase ER stress which initiate caspase activation and apoptosis which lead to mitochondrial damage via ROS production<sup>[47]</sup>, destruction of apical microvilli and necrosis of cells may explain decrease in alkaline phosphatase activity (a marker enzyme of brush border membrane of proximal tubular cells)<sup>[48]</sup> seen in our results in GA3 treated group which is in agreement with<sup>[49]</sup> who revealed decrease in enzyme activity in brush border of convoluted tubules of renal cortex due to deep hypotonic circulatory arrest. Many lysosomes seen in degenerated tubular cells was explained by<sup>[50]</sup> as accelerated intracellular degeneration of macromolecules.

Podocyte showed irregular nucleus, dilated RER and fused foot processes. These changes were similar to findings of<sup>[50]</sup> who explained damage as one of features of proteinuric glomerular diseases. Podocytic injury may be due to its cytoskeleton, as one of early changes was down relation of actin associated protein synaptopodin<sup>[51]</sup>.

Our histological and immunohistochemical results showed marked improvement with administration of antioxidant CoQ10 with GA3, as stated by<sup>[52]</sup> that CoQ10 can eradicate free radicals to improve health. Several studies revealed this improvement due to reduction in lipid peroxidation with decrease in MDA level, enhancement of scavenging ability and restoration of antioxidant defense system by increase SOD and CAT levels. Also, CoQ10 is capable to relief stress conditions as oxidative stress and ER stress<sup>[53]</sup>. It was reported that CoQ10 was used as a potential therapy to inhibit progression of lung and liver fibrosis by decreasing different inflammatory mediators as MCP1, TGF- $\beta$  and TNF. Moreover, CoQ10 might protect cell membrane phospholipid, mitochondrial membrane protein against oxidative damage<sup>[54]</sup>. Also, it plays a substantial role in production of intracellular energy, improvement of endothelial dysfunction and activating mitochondrial uncoupling proteins<sup>[55]</sup>. It also, could inhibit leucocytic infiltration, and glomerulosclerosis in diabetic animals<sup>[56]</sup>. So, CoQ10 could attenuate the detrimental effect of GA3 on the kidney.

#### CONFLICT OF INTERESTS

There are no conflicts of interest.

#### REFERENCES

1. Fishel FM. (2006): Gibberellins. Agronomy department, Florida cooperative extension service, Institute of food and agricultural sciences, University of Florida, USA.
2. Ashikari M, Sakakibara H, Lin S, Yamamoto T, Takashi T, Nishimura A *et al.*(2005): Cytokinin oxidase regulates rice grain production. *Science*, 309:741-745.
3. Neil AC, Reece JB.(2002): Phytohormones (plant hormones) and other growth regulators: Gibberellin. In: biology. 6th ed., San Francisco, Benjamin Cummings.
4. Sakr SA, Okdah YA and El-Abd SF.( 2003): Gibberellin A3 induced histological and histochemical alterations in the liver of albino rats. *Science Asia*, 29: 327-331.
5. Tomlin CDS.(2004): Gibberellic acid. In: The e-Pesticide Manual. 13 ed., edited by Tomlin, C.D.S. (Hampshire, UK, British Crop.Protection Council); Chapter 3, 5.
6. Celik I, Tuluze Y, Isik I. (2007): Evaluation of toxicity of abscisic acid and gibberellic acid in rats 50 days drinking water study. *Journal of Enzyme Inhibition and Medical Chemistry*; 2:219-226.
7. Battino M, Ferreiro MS, Bomparde S, Leone L, Mosca F, Bullon P. (2001): Elevated hydroperoxide levels and antioxidant patterns in Papillon-Lefevre syndrome. *JPeriodontol*.72:1760-6.
8. Wilson M, Newman N, Bullon P.(1999): Oxidative injury and inflammatory Periodontal diseases:The challenge of antioxidants to free radicals and reactive oxygen species. *Crit Rev Oral Biol Med*.10:458-76.
9. Saini R,Saini S, Sharm S.(2010): Antioxidants accelerates cellular health. *Int J Green Pharm*. 3:212.
10. Shekelle P, Morton S, Hardy ML. (2003): Effect of supplemental antioxidants vitamin C, vitamin E and coenzyme Q10 for the prevention and treatment of cardiovascular disease. *EvidRepTechnolAssess*;83:1-3.
11. Celikezen F.C, Oto G, Ozdemir H, Kmouroglu A, Yoruk I, Demir H, Yeltekin A.(2015): The antioxidant effect of boric acid and CoQ10 on pulmonary fibrosis in bleomycin induced rats. *J. Sci. Technol.*, 2,pp.27-31.
12. Erin N, Afacan B, Erosy Y, Ercan F, Balci MK. (2008): Gibberellic acid, a plant growth regulator, increases mast cell recruitment and alters substance P levels. *Toxicology*; 254:75-81.
13. Keiding R, Horder M, Gerhardt W. (1974): Recommended methods for the determination of four enzymes in blood. *Scand J Clin Lab Invest*; 33:291-306.
14. Nishikimi M, Rao NA, Yog K (1972): Colorimetric determination of superoxide dismutase activity. *Biochem. Biophys. Res. Commun* 46: 849-851.
15. Aebi H.(1984): Catalase in Vitro. *Methods in Enzymology*; 105: 121-126.
16. Ohkawa H, Nobuko O, Yagi K (1979): Assay for lipid peroxides in animal tissues by thiobarbituric acid reaction *Analytical Biochemistry*; volume 95 Issue 2, pages 351-358.
17. Bancroft JD and Layton, C. (2010): Theory and practice of histological technique, 7th ed., London: Churchill Livingstone. P 173-214.
18. Drury RAB and Wallington EA.(1980): Carlton's histological techniques. 5th ed. Oxford: university Press.

19. Pollock I, Rampling D, Greenwal SE, Malone M.(1995): Desmin expression in rhabdomyosarcoma: Influence of the Desmin Clone and Immunohistochemical Method. *J Clin Pathol*1995; 48(6):535-538.
20. Van Noorden S and Polak M. (2014): *Immunocytochemistry : practical applications in pathology and biology*. 2nd ed. Melbourne, London, Edinburgh and New York: Churchill Livingstone; PP. 31-40.
21. Allegranza A, Girlando S, Arrigoni GL, Veronesi s, Mauri FA.(1991): Proliferating cell nuclear antigen expression in central nervous system neoplasms. *Virchows Arch APatholAnatHistopathol*; 419(5):417-423.
22. Glauert AM and Lewis PR.(1999): *Biological specimen preparation for transmission electron microscope*. 1<sup>st</sup> ed. London: Princeton University Press.
23. Peat, J and Barton, B. (2005): *Medical statistics. A Guid to data analysis and critical appraisal*. First ed., Wiley-Blackwell.113-19.
24. Saber NA and Jane B. (2003): *Biology*. 6th ed. San Francisco, USA: Benjamin Cumming; 2003. p. 141–155.
25. Martinez C, Lopez FJ, Lopez JM. (2007): Reviews in Mechanistic Toxicology, Glomerular nephrotoxicity of amino glycosides. *ToxicolApplPharmacol*. 128(7):220-227.
26. El-Moghazy M, Zedan N., El-Atrsh A, El-Gogary M, Tousson E. (2014):The possible effect of diets containing fish oil (omega-3) on hematological, biochemical and histopathological alterations of rabbit liver and kidney. *Biomedicine and Preventive Nutrition*.4:371-377.
27. Yazar S and Baydan E.(2008): The subchronic toxic effects of plant growth promoters in mice. *Ankara Univ Vet FakDerg*;55(1):17–21.
28. Wakamatsu N, Surdyk K, Carmichael KP, *et al.* (2007): Histologic and ultrastructural studies of juvenile onset renal disease in four Rottweiler dogs. *Vet Pathol*. 44(1):96–100.
29. Takahashi M, Morita T, Sawada M, Uemura T, Haruna A, Shimada A. (2005): Glomerulocystic kidney in a domestic dog. *J Comp Pathol*. 133:205–208.
30. Troudi A, Samet AM, Zeghal N. (2010): Hepatotoxicity induced by gibberellic acid in adult rats and their progeny. *ExpToxicolPathol*; 62:637–642
31. Troudi A, Ben AI, Soudani N, *et al.* (2011): Oxidative stress induced by gibberellic acid on kidney tissue of female rats and their progeny: biochemical and histopathological studies. *J PhysiolBiochem*. 67(3):307–316.
32. Borni A, Mariem C, AwatefEj, Malek G, Kamel J, Hela M, Tahia B, Hanen K, Najiba Z. (2018): Effects of co-exposure to imidacloprid and gibberellic acid on redox status, kidney variables and histopathology in adult rats.*ArchPhysiolBiochem*. 124(2):175-184.
33. Stadtman E.R and R. L. Levine. (2000): *Ann. N. Y. Acad. Sci*. 2000, 899, 191.
34. Lam, M., Dubyak, G., Chen, L., Nuñez, G., Miesfeld, R. L. and Distelhorst, C. W. (1994) Evidence that BCL-2 represses apoptosis by regulating endoplasmic reticulum-associated Ca<sup>2+</sup> fluxes. *Proc. Natl. Acad. Sci. U S A* 91; 6569–6573.
35. Karch J, Kwong J. Q., Burr A. R., Sargent M. A., Elrod J. W., Peixoto P. M, Martinez-Caballero S, Osinska H, Cheng E. H., Robbins J, Kinnally K. W, Molkentin J. D. (2013): Bax and Bak function as the outer membrane component of the mitochondrial permeability pore in regulating necrotic cell death in mice. *Elife*.27;2:e00772.
36. Whelan R, Konstantinidis, K., Wei A, Chen Y, Reyna, D, Jha S, Yang, Y, Calvert J, Lindsten T, Thompson C, Crow M, Gavathiotis E, Dorn G. *et al.* (2012) Bax regulates primary necrosis through mitochondrial dynamics. *Proc. Natl. Acad. Sci. U. S .A*. 109; 6566–6571.
37. Al Drees I, Mahmoud S, Mona S. (2017): Histological and Immunohistochemical Basis of the Effect of Aminoguanidine on Renal Changes Associated with Hemorrhagic Shock in a Rat Model *ActaHistochem. Cytochem*. 50 (1): 11–19.
38. Ehab T, Afaf A, Mervat M, Abdallah A. (2019): Histopathological and immunohistochemical studies on the effects of Ethephon on liver and kidney in male rats. *International Journal of Pathology and Biomarkers*, Vol.1, No.1, P.1-6.
39. Thomas GL, Yang B, Wagner BE, Savill J, El Nahas AM (1998): Cellular apoptosis and proliferation in experimental renal fibrosis. *Nephrol DialTransplant* 13: 2216–2226.
40. Qin W, Xu Z, Lu Y, Zeng C, Zheng C. (2012): Mixed organic solvents induce renal injury in rats. *PLoS.One* 2012; 7: e45873, 11pages.
41. Miki N, Shigeru S, Shigetaka Y, Takashi N, Takanari G, Toshiro F.(2006 ): Podocyte Injury Underlies the Glomerulopathy of Dahl Salt-Hypertensive Rats and Is Reversed by Aldosterone Blocker.*HYP*.47(6):1084-93.
42. Haiting H, Xu L, Yanwu C, Tang X, GuMeiying H. *et.al.* (2017): Inhibition of TRPC6 Signal Pathway Alleviates Podocyte Injury Induced by TGF-β1. *Cell Physiol Biochem*. 41(1):163-172.
43. Walaa A, Asmaa S, Manar Faried. (2019): Green tea extract protects the renal cortex against bisphenol A-induced nephrotoxicity in the adult male albino rat: a histological and immunohistochemical study. *Eur. J. Anat*. 23 (6): 415-424.
44. Eto N, Wada T, Inagi R, Takano H, Shimizu A, Kato H. *et al.* (2007): Podocyte protection by darbepoetin: preservation of the cytoskeleton and nephrin expression. *Kidney Int*;72:455-463.

45. Abdel Rahman MA, Abdel Atty YH, Abdel Rahman MM, Sabry M.(2017): Structure changes induced by gibberellic acid in the renal cortex of adult male albino rats. *MOJ Anta Physiol*; 3:21-27.
46. Dixit SG, Rani P, Anand A, Khatri K, Chauhan R, Bharihoke V. (2014): To study the effect of monosodium glutamate on histomorphometry of cortex of kidney in adult albino rats. *Ren Fail* 2014; 36:266–270.
47. Rasheva VI and Domingos PM. (2009): Cellular responses to endoplasmic reticulum stress and apoptosis. *Apoptosis* 14: 996–1007.
48. Ujjawal S, Deeksha P, Shrawan K, Singh b. *et al.* (2014): Reduced L/B/K alkaline phosphatase gene expression in renal cell carcinoma: Plausible role in tumorigenesis. *Biochimie*. 104:27-45.
49. trumper L, Coux G, Elias MM., Effect of acetaminophen on Na, K ATPase and alkaline phosphatase on plasma membrane of renal proximal tubules. *Toxicol Appl Pharmacol* 2000; 164:143-148.
50. Sayed H, Hoda A, Heba M, Martha A. (2019): Effects of exposure to gibberellic acid during pregnancy and lactation on the postnatal development of the renal cortex in the albino rat. *JCMRP*. 4(2):121-130.
51. Scott J. Harvey, George J, Jeanette C, Seth G, Bernhard S, Brian D *et al.* (2008): Podocyte-Specific Deletion of Dicer Alters Cytoskeletal Dynamics and Causes Glomerular Disease. *J Am Soc Nephrol*. 19(11):2150-8.
52. Ochoa J, Quiles J, Huertas J, Mataix J. (2005): Coenzyme Q10 protects from aging-related oxidative stress and improves mitochondrial function in heart of rats fed a polyunsaturated fatty acid (PUFA)-rich diet. *J Gerontol A Biol Sci Med Sci*. 60(8):970-5.
53. Tarry-Adkins J, Fernandez-Twinn D, Hargreaves I, Neergheen, V. (2016): Coenzyme Q10 prevents hepatic fibrosis, inflammation and oxidative stress in a rat model of poor maternal nutrition and accelerated postnatal growth. *Am. J. Clin. Nutr.* 103(2), pp. 579-588.
54. Lee B-J, Tseng Y-F, Yen C, Lin P. (2013): Effects of coenzyme Q10 supplementation on antioxidation and anti-inflammation in coronary artery disease patients during statins therapy: a randomized, placebo-controlled trial. *Nutr J*. 12(1):142.
55. El-Sheikn AAK, Morsy MA, Mahmoud MM, Rifaai RA, Abdelrahman AM. (2012): Effect of coenzyme Q10 on doxorubicin induced nephrotoxicity in rats. *Adv Pharmacol Sci*. 2012;8.doi:10.1155/2012/981461.
56. Rosenfeldt FL, Haas SJ, Krum H. (2007): Coenzyme Q10 in the treatment of hypertension: a meta-analysis of the clinical trials. *J Hum Hypertens*. 21(4):297–30.

## الملخص العربي

# دراسة بالميكروسكوب الضوئي والإلكتروني عن تأثير حمض الجبريليك على القشرة الكلوية لذكور الفئران البيضاء البالغة والدور الوقائي المحتمل للإنزيم المساعد

أميرة فهمي علي<sup>١</sup>، نجوي سعيد غنيم<sup>١</sup>، رشا ممدوح سلامة<sup>٢</sup>

<sup>١</sup> قسم الأنسجة- كلية الطب- جامعة المنوفية

<sup>٢</sup> قسم التشريح والأجنة- كلية الطب- جامعة المنوفية

**المقدمة:** حمض الجبريليك هو منظم نمو النبات، يستخدم لزيادة حجم النبات وإنتاجه وتوافره على مدار العام. ومع ذلك، يجب استخدامه بحذر لتقليل سميته المحتملة لبعض أجزاء الجسم بما في ذلك الكلى. الإنزيم المساعد Q10 هو عنصر غذائي يظهر بشكل طبيعي في الجسم. كما أنه يوجد في العديد من الأطعمة ويعمل كمضاد للأكسدة، والذي يحمي الخلايا من التلف ويلعب دورًا مهمًا في عملية التمثيل الغذائي للخلايا.

**الهدف من البحث:** معرفة تأثير حمض الجبريليك على الكلى والتأثير الوقائي المحتمل للإنزيم المساعد Q10 في الفئران. **مواد وطرق البحث:** تم استخدام أربعين من الفئران الذكور البالغين في الدراسة الحالية. تم تقسيم الفئران إلى أربع مجموعات، المجموعة الأولى (المجموعة الضابطة)، المجموعة الثانية (المجموعة المعالجة بالإنزيم المساعد Q10)، المجموعة الثالثة (المجموعة المعالجة بحمض الجبريليك) والمجموعة الرابعة (المجموعة المعالجة بالإنزيم المساعد Q10 وحمض الجبريليك). في نهاية التجربة، تم جمع عينات الدم لقياس مستويات اليوريا والكرياتينين، وتمت معالجة أنسجة الكلى لدراسة بيوكيميائية ودراسة بالميكروسكوب الضوئي والإلكتروني.

**النتائج:** كشفت المجموعة المعالجة بحمض الجبريليك عن تلف واضح في الكبيبات وزيادة قطر الأنابيب الكلوية. وزيادة سمك الغشاء القاعدي، مع ضمور واضح في الكبيبات وزيادة قطر الأنابيب. كما أظهرت بعض الخلايا الأنبوبية تجويفات سيتوبلازمية ونوى حلقية. ولوحظ تجويف ببعض الأنابيب الكلوية ونزيف وارتشاح خلالى شديد. وكشفت الدراسة البيوكيميائية زيادة مستوى اليوريا والكرياتينين، وزيادة في مستوى MDA وانخفاض كبير في مستوى SOD و CAT مقارنة بالمجموعة الضابطة. وقد تحسنت التغيرات السابق ذكرها بإضافة الإنزيم المساعد Q10. **الاستنتاج:** الإنزيم المساعد Q10 يمكن أن يحمي من السمية الكلوية الناتجة من حمض الجبريليك.